materials

MDPI

Article

Incorporation of Mixing Microbial Induced Calcite Precipitation (MICP) with Pretreatment Procedure for Road Soil Subgrade Stabilization

Xiaodi Hu[1], Xiongzheng Fu[1], Lirong Lin[1], Pan Pan[1],*, Yihan Sun[2]

[1] School of Civil Engineering and Architecture, Wuhan Institute of Technology, Wuhan Hubei, 430205, China ; huxiaodi625@hotmail.com (X.H.); fxzxfxzxf@gmail.com (X.F.); linlirong802@163.com (L.L.)

[2] Zhejiang Academy of Transportation Sciences, Hangzhou, Zhejiang, 310023, China.; sunyh@whut.edu.cn

* Correspondence: panpan8597@126.com; panp@wit.edu.cn

Abstract: Microbial induced carbonate precipitation (MICP) provides an alternative method to stabilize the soil. To further improve the reinforcement effect, this study aims to propose a strategy by incorporating the mixing MICP method with pretreatment procedure. A series of laboratory tests were performed to investigate the preparation parameters, the engineering properties, the $CaCO_3$ distribution as well as the mineralogical and micro structural characteristics of pretreatment-mixing MICP reinforced soil (PMMRS). Based on the orthogonal experiment results, the optimum preparation parameters for PMMRS were determined. The UCS of PMMRS was more strongly dependent on the moisture content and concentration of $CaCl_2$ than the concentration ratio of $CaCl_2$ to urea. Moreover, it was testified that incorporation of pretreatment procedure improved the stabilization effect of traditional mixing MICP method on the clayed sand (CLS). The UCS of PMMRS specimen was increased by 198% and 78% than the pure CLS and the simple mixing MICP reinforced soil, respectively. Furthermore, the $CaCO_3$ products generated consisted of the aragonite, calcite and vaterite, which distributed unevenly inside the specimen no matter the lateral or vertical direction. The reason might be that oxygen content varied with the regions in different directions and hence affected the mineralization reaction. In addition, the mineralization reaction would affect the pore structure of the soil, which was highly related to the reinforcement effect of MICP reinforced soil.

Keywords: microbial induced calcite precipitation (MICP); pretreatment-mixing MICP method; subgrade soil stabilization

Citation: Lastname, F.; Lastname, F.; Lastname, F. Title. *Materials* **2022**, *15*, x. https://doi.org/10.3390/xxxxx

Academic Editor: Firstname Lastname

Received: date
Accepted: date
Published: date

Publisher's Note: MDPI stays neutral with regard to jurisdictional claims in published maps and institutional affiliations.

Copyright: © 2022 by the authors. Submitted for possible open access publication under the terms and conditions of the Creative Commons Attribution (CC BY) license (https://creativecommons.org/licenses/by/4.0/).

1. Introduction

With the rapid development of economy and society, there is a continually increasing demand for road construction in China during the past decades. By the end of 2020, the total road mileage reached to 5,198,100 km ~~in China~~. Since China is a vast country, the geological conditions might vary significantly ~~with the~~ regions. For some projects, it is usually encountered that the engineering properties of soil cannot meet the specification requirements. In order to ensure the safety and durability of road structure, effective methods are needed to eliminate the potential risk caused by the poor soil.

Generally, there are four common techniques to reinforce the road soil subgrade, including: (a) using natural or synthetic materials, e.g. geosynthetics, fibers, polyester, and etc. [1]; (b) physical engineering methods, e.g. replacing the situ poor soil, dynamic compaction, using sand/stone columns, and etc. [2]; (c) injecting/grouting chemical materials, e.g. micro-fine cement, epoxy, phenoplasts, silicates, polyurethane, and etc. [3,4]; (d) inorganic binder stabilization, e.g., Poland cement, lime, coal ash, and etc. [5,6]. Among these methods, replacing the situ poor soil and cement binder stabilization are

the most common in China, but have considerable disadvantages that needed to be seriously considered. On the one hand, replacing the situ soil method is expensive and low efficiency, although it seems to be the simplest. The alternative soil that meets the technical specification requirement needs to be explored and transported from somewhere else, while the replaced poor soil is needed to be removed and requires a large amount of land for disposal. It will bring considerable negative effects on the ecological environment as well. On the other hand, the cement binder stabilization is not so environmentally friendly since cement production consumes a large amount of energy and significantly increases CO_2 emissions [7,8]. Therefore, it is urgent to develop a more environmentally friendly and efficient method for stabilizing the poor soil subgrade.

Microbial Induced Calcite Precipitation (MICP), which is an emerging and eco-friendly technique based on the microbial mineralization, has been developed and applied in the soil reinforcement [9], permeability reduction [10], slopes stabilization [11], surface reparation [12], liquefaction resistance enhancement [13], and heavy metal pollution treatment [14]. According to the reaction principles, microbial mineralization process of the MICP can be divided into several categorizes, e.g., urea hydrolysis, denitrification [15], iron reduction, enzymatic-induced carbonate precipitation (EICP) [16]. Among them, the urea hydrolysis MICP has gained the most attentions due to the quickly controllable reaction, high chemical conversion efficiency and excellent environmental tolerance. Moreover, Sporosarcina pasteurii, which is widely lived in natural soil, has high urease activity and becomes one of the most popular MICP bacteria specie nowadays [17]. The main chemical reactions of urea hydrolysis MICP are summarized as follows [18], while the urea hydrolysis reaction is catalyzed by the carbonic anhydrase and urease [19].

$$CO(NH_2)_2+H_2O \rightarrow NH_3+NH_2COOH \quad (1)$$

$$NH_2COOH+H_2O \rightarrow H_2CO_3+NH_3 \quad (2)$$

$$NH_3+H_2O \leftrightarrow NH_4^++OH^- \quad (3)$$

$$H_2CO_3 \rightarrow HCO_3^-+H^+ \quad (4)$$

$$H_2CO_3 \rightarrow HCO_3^-+H^+ \quad (5)$$

For reinforcing soil, the application of MICP can be divided into four categories, including injecting [20] or pre-injecting method [21], spraying method [22], soaking method [23,24], and mixing method [25,26]. For the injecting/pre-injecting, spraying and soaking methods, the bacteria and cement substances are needed to diffuse from the surface to inside or from one side to the opposite. In this case, the $CaCO_3$ generated by the mineralization reaction might block the pore throat and prevent the microorganisms bacteria and cement substances from diffusing, which would attenuate the reinforcement effect of MICP method [27,28]. From this point of view, these methods are only suitable for enhancing the coarse-grained soil, but have limited reinforcement effect on the fine-grained soil with dense structure. Compared to these methods, mixing MICP can lead soil particles contacting well with the bacteria and cement substances, and hence shows considerable advantages in treating both coarse-grained and fine-grained soil. Moreover, mixing MICP requires fewer bacteria, less cement substances and shorter treatment period. Therefore, it is recognized that the mixing method is more prospective for the large-scale soil treatment, such as road soil subgrade, mine backfilling and so on.

As known, the maximal dry density and optimum moisture content are the critical parameters for soil compaction. The optimum moisture content of soil would limit the amount of solution containing the microorganisms and cement substances, which determines the reinforcement effect of mixing MICP method. Moreover, it is hard to pre-

pare the solution with high concentration and high activity bacterial during the mixing process as well. On the other hand, the MICP process would consume a considerable amount of calcium. However, high concentration of calcium ion in solution would degrade the urease activity and thus attenuates the chemical conversion efficiency of MICP [9]. Consequently, the combination effects might lower the production of $CaCO_3$ and minimize the reinforcement effect of mixing MICP method. Therefore, it is necessary to modify the traditional mixing MICP method for further application in road soil treatment.

This study aims to propose a strategy by incorporating the mixing MICP method with pretreatment procedure, which is expected to add more substances involved in the mineralization reaction without increasing the concentration of the cementation solution and bacterial solution. Firstly, orthogonal experiment was employed to obtain the optimum parameters for preparing the pretreatment-mixing MICP reinforced soil (PMMRS). Moreover, the engineering performance of PMMRS was evaluated by the unconfined compressive strength (UCS) test and the unconsolidated-undrained triaxial (UU) test, while the content and distribution of $CaCO_3$ generated were analyzed by the acid wash method. Furthermore, the PMMRS was studied by the field emission scanning electron microscope (FESEM), X-Ray Diffraction (XRD) and mercury injection apparatus (MIA) as well.

2. Materials and Methods

2.1 Soil

In this study, the soil, which was a kind of clayey sand (CLS), was obtained from an engineering project in Hong'an City, China. The particle within 0.075mm was analyzed by a laser particle sizer (Malvern Mastersizer 2000), while the particle greater than 0.075mm by the water washing method according to the Chinese Specification JTG 3430-2020. ~~Figure 1 presents the size distribution of the CLS.~~ The physical properties of the CLS were tested according to the JTG 3430-2020 and the results are shown in Table 1.

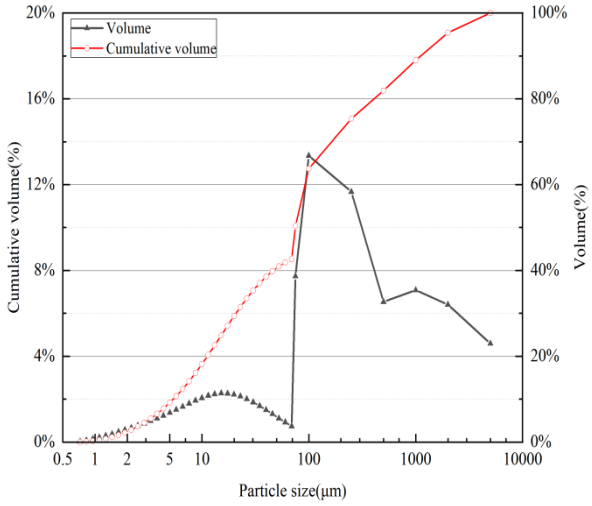


Figure 1. Particle size distribution of the CLS

Table 1. Physical properties of the CLS

Indexes	Results	Indexes	Results
Classification	Clayey Sand (CLS)	Clay	9.20%
Liquid limit	46.52%	Silt	40.44%
Plastic limit	25.61%	Sand	50.36%
Plastic index	20.91	d_{10}	0.0054mm

Specific gravity	2.71	d_{30}	0.0209mm
Maximum dry density	2.09g/cm^3	d_{60}	0.9801mm
Optimum moisture content	9.2%	C_u	181.3474
pH	6.87	C_s	0.0821

118 2.2 Bacteria Culture for MICP

119 The Sporosarcina pasteurii was obtained from the China General Microbiological
120 Culture Collection Center (CGMCCC) with strain numbers of ATCC-11859 and CGMCC
121 1.3687. The liquid culture medium was augmented with 20 g/L urea, 20 g/L tryptone, 5
122 g/L soy peptone, 5 g/L NaCl, and 24 mg/L NiCl2 while the pH value of liquid was con-
123 trolled as 8.0. After the sterile and inoculation treatment, the bacteria-bearing liquid
124 culture medium was cultured in an oscillating incubator at 30oC with a vibration rate of
125 180 rpm for 24 hours. The number of microorganisms in the bacterial solution was
126 measured by the 721G visible spectrophotometer with a wavelength of 600nm, and the
127 OD600 of bacteria solution was kept at about 1.2.

128 2.3 Cementation Solution and Water

129 The $CaCl_2$ and $CO(NH_2)_2$ was used to prepare the cementation solution. The $CaCl_2$
130 has five concentration levels (1.0, 2.0, 3.0, 4.0, and 5.0 mol/L) and the concentration ratios
131 of $CaCl_2$ to $CO(NH_2)_2$ were 1:1, 1:2, 1:3, 2:1, and 3:1, respectively. The water used to pre-
132 pare the liquid culture medium and cementation solution was the deionized water, and
133 the rest was tap water unless otherwise noted.

134 2.4 Sample Preparation

135 2.4.1 Soil Pretreatment

136 In this study, the CLS was pretreated with the cementation solution by three steps.
137 Firstly, the amount of cementation solution was determined based on the mass and
138 moisture content of the CLS. Secondly, the CLS was mixed uniformly with the cementa-
139 tion solution for 5 minutes. Finally, the mixed CLS was dried till the constant weight at
140 105°C.

141 2.4.2 Specimen Preparation and Curing

142 For the UCS test, the cylindrical specimens with a diameter of 50mm and a height
143 of 50mm were prepared. Figure 2 illustrates the preparation procedure for the UCS
144 specimen. Firstly, the inner wall of the mold was coated with petroleum jelly to prevent
145 the CLS from sticking to the mold. Secondly, the pretreated CLS was mixed with the
146 bacteria solution, and then filled in the mold. The CLS mixture was compacted until two
147 blocks were pressed into both the sides of the mold. Finally, the compacted specimens
148 were demoulded and then cured in a biological incubator at 30oC within different cur-
149 ing time before further tests.

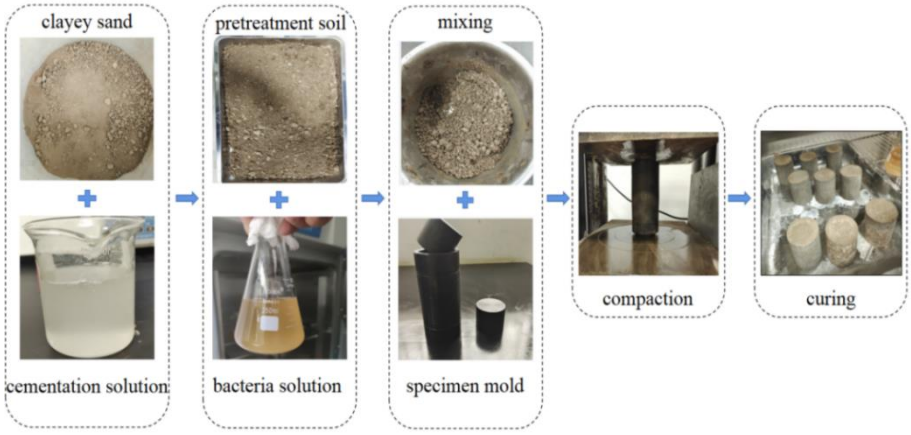


Figure 2. The specimen preparation of UCS test

For the UU test, the specimens with a diameter of 39.1 mm and a height of 80 mm were compacted with a hammer in four layers. Each layer should be compacted well before adding CLS mixture for the next layer. The subsequent preparation and curing procedures were similar with the UCS specimen.

2.5 Test Method

2.5.1 Unconfined Compressive Strength (UCS)

In this study, the UCS test was conducted with a loading rate of 1 mm/min by the universal testing machine (UTM-100). The sizes of the cured specimens were measured before test.

2.5.2 Undrained-Unconsolidated (UU) triaxial test

The UU test was performed by the triaxial testing machine. Firstly, the cured specimens were vacuum saturated for 24 hours before test. In this study, the specimen was axially loaded with a rate of 0.4mm/min under three fixed pressure levels, including 100kPa, 200kPa and 300kPa, respectively. The test was finished when the axial strain reached to 20%.

2.5.3 Content and distribution of $CaCO_3$

The content and distribution of $CaCO_3$ in the PMMRS specimens was investigated by the acid washing method [29]. In order to ensure the sampling representation, the samples were obtained from nine locations of the specimen. Figure 3 illustrates the sampling strategy considering both the lateral and vertical directions.

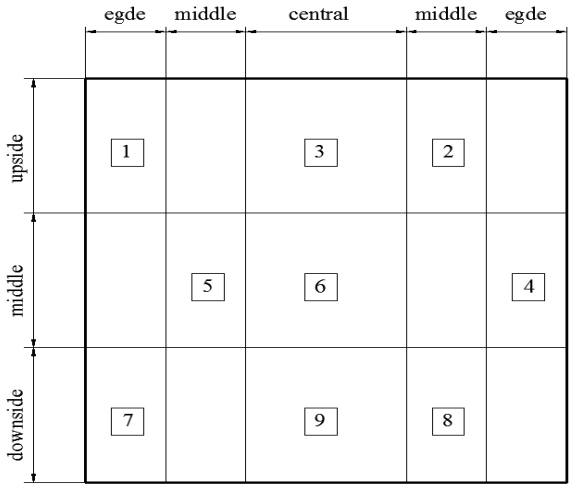


Figure 3. Strategy for obtaining the CCC sample

Before test, the sample was firstly washed by the deionized water to remove the soluble salts and then dried to a constant mass m_a. Secondly, the dried sample was washed by the HCl solution several times until all the $CaCO_3$ reacted with the HCl. Finally, the sample was washed by the deionized water again to remove the calcium and then dried to a constant mass m_b. The content of $CaCO_3$ (CCC) of sample can be calculated by Eq. (6).

$$CCC = (100 - \frac{m_b}{m_a}) * 100\% \quad (6)$$

2.5.4 X-ray Diffraction (XRD)

The mineralogical composition of the pure CLS and PMMRS were measured by the X-ray diffractometer (D8 ADVANCE). The samples were dried at 105°C for 12h and then pulverized to pass through the 0.075mm sieve. During the test, the scanning speed was 3° per minute and the scanning angle was from 10° to 80° in units of 2-theta.

2.5.5 Field Emission Scanning Electron Microscope (FESEM)

A Zeiss GminiSEM 300 FFESEM was employed to analyze the morphology and distribution of $CaCO_3$ in the CLS, which can be further used to investigate the bonding characteristics between the CLS particles. The samples obtained from the cyclic specimen were needed to smooth the surface and dried at 105°C for 12h before test.

2.5.6 Mercury Injection Apparatus (MIA)

The particle and pore structure characteristics inside the specimens were investigated by the mercury injection apparatus (AutoPore Iv 9520). Cubic samples with a length of 15 mm were taken from the specimens. All the samples were smoothed and dried at 105°C for 12h before test.

2.6 Orthogonal Experiment Design

In this study, orthogonal experiment was used to investigate the different factors that influence the reinforcement effect of pretreatment-mixing MICP method, including the maximal dry density and optimum moisture content of the CLS, the calcium ion concentration, and the ratio of $CaCl_2$ to urea in the cementation solution. Since the dry density of CLS is quantitatively determined by the moisture content, the moisture content can be considered as a factor that represents the dry density. Therefore, the orthog-

onal experimental was designed with three parameters and five levels as in Table 2. The unconfined compressive strength was adopted as the evaluation indicator for the orthogonal experiment. Before the UCS test, the samples for each group were cured at 30° C for 7 days and then dried at 105°C for 24h. To ensure the accuracy, six duplicate samples were prepared for each group and the corresponding average value were used for the statistical analysis.

Table 2. The orthogonal experiment design

Group Number	Moisture Content(%)	Concentration of $CaCl_2$ (mol/L)	Ratio of $CaCl_2$ to Urea	Empty Column	Empty Column	Empty Column
1	(1) 13%	(1) 2.0	(1) 1:2	(1) -	(1) -	(1) -
2	(1) 13%	(2) 4.0	(3) 2:1	(4) -	(5) -	(2) -
3	(1) 13%	(3) 3.0	(5) 1:3	(2) -	(4) -	(3) -
4	(1) 13%	(4) 5.0	(2) 1:1	(5) -	(3) -	(4) -
5	(1) 13%	(5) 1.0	(4) 3:1	(3) -	(2) -	(5) -
6	(2) 10%	(1) 2.0	(5) 2:1	(4) -	(3) -	(5) -
7	(2) 10%	(2) 4.0	(2) 1:3	(2) -	(2) -	(1) -
8	(2) 10%	(3) 3.0	(4) 1:1	(5) -	(1) -	(2) -
9	(2) 10%	(4) 5.0	(1) 3:1	(3) -	(5) -	(3) -
10	(2) 10%	(5) 1.0	(3) 1:2	(1) -	(4) -	(4) -
11	(3) 11%	(1) 2.0	(4) 1:3	(2) -	(5) -	(4) -
12	(3) 11%	(2) 4.0	(1) 1:1	(5) -	(4) -	(5) -
13	(3) 11%	(3) 3.0	(3) 3:1	(3) -	(3) -	(1) -
14	(3) 11%	(4) 5.0	(5) 1:2	(1) -	(2) -	(2) -
15	(3) 11%	(5) 1.0	(2) 2:1	(4) -	(1) -	(3) -
16	(4) 9%	(1) 2.0	(3) 1:1	(5) -	(2) -	(3) -
17	(4) 9%	(2) 4.0	(5) 3:1	(3) -	(1) -	(4) -
18	(4) 9%	(3) 3.0	(2) 1:2	(1) -	(5) -	(5) -
19	(4) 9%	(4) 5.0	(4) 2:1	(4) -	(4) -	(1) -
20	(4) 9%	(5) 1.0	(1) 1:3	(2) -	(3) -	(2) -
21	(5) 12%	(1) 2.0	(2) 3:1	(3) -	(4) -	(2) -
22	(5) 12%	(2)4.0	(4) 1:2	(1) -	(3) -	(3) -
23	(5) 12%	(3) 3.0	(1) 2:1	(4) -	(2) -	(4) -
24	(5) 12%	(4) 5.0	(3) 1:3	(2) -	(1) -	(5) -
25	(5) 12%	(5) 1.0	(5) 1:1	(5) -	(5) -	(1) -

3. Results and Discussion

3.1 Orthogonal Experiment Results

The specimens for different PMMRS groups were tested and the corresponding average UCS is summarized in Table 3. The combination effects of moisture content, concentration of $CaCl_2$, and the ratio of $CaCl_2$ to urea have a considerable effect on the UCS of PMMRS. For example, the average UCS of specimens for the No.18 group (moisture content 9%, concentration of $CaCl_2$ 3mol/L, and the ratio of $CaCl_2$ to urea 1:2) was 12.92MPa, which was 5.2 times than the No.15 group (moisture content 11%, concentration of $CaCl_2$ 3mol/L, and the ratio of $CaCl_2$ to urea 2:1).

Table 3. The orthogonal experiment results

Group Number	Average UCS (MPa)	Group Number	Average UCS (MPa)
1	3.43	14	5.92
2	5.22	15	2.46

3	6.02	16	8.89
4	9.31	17	12.14
5	4.32	18	12.92
6	5.43	19	9.42
7	8.62	20	7.65
8	9.88	21	4.90
9	6.56	22	6.04
10	4.32	23	10.20
11	5.15	24	3.25
12	8.11	25	4.06
13	6.97		

The range analysis was used to determine the optimum parameters for the pre-treating-mixing MICP process, and the results are shown in Table 4. The K_i is the sum of the average UCS results for the level i in each column. Since UCS represents the engineering property of PMMRS, the level corresponding to the maximum K_i in each column was adopted to determine the optimum parameters for preparing the PMMRS specimen. Therefore, the moisture content was determined as 9%, the concentration of $CaCl_2$ 3.0 mol/L, and the concentration ratio of $CaCl_2$ to urea 1:1. In addition, when the moisture was 9% by weight of the CLS, the corresponding maximum dry density was 2.09g/cm^3.

As shown in Table 4, the UCS of PMMRS decreased with the moisture content. When the moisture content increased from 9% to 13%, the dry density of PMMRS decreased from 2.09g/cm^3 to 1.98g/cm^3, leading to the strength of PMMRS decreasing. Since high concentration of calcium ion would degrade the activity of urease, the UCS of PMMRS increased initially with the concentration of $CaCl_2$ in the cementation solution and then showed a decrement trend when the $CaCl_2$ concentration was greater than 3mol/L.

Table 4. The orthogonal experiment analysis table

Group Number	Moisture Content	Concentration of $CaCl_2$ (mol/L)	Ratio of $CaCl_2$ to Urea
K_1	(13%) 28.30	(2.0) 27.80	(1:2) 35.95
K_2	(10%) 34.81	(4.0) 40.13	(1:1) 38.21
K_3	(11%) 28.61	(3.0) 45.99	(2:1) 28.65
K_4	(9%) 51.02	(5.0) 34.46	(3:1) 34.81
K_5	(12%) 28.45	(1.0) 22.81	(1:3) 33.57
R	22.72	23.18	9.56

Furthermore, the range value R was used to evaluate the effect significance of the preparation parameters on the UCS, which was calculated by Eq. (7). The greater the R value, the more significant the parameter. As shown in Table 4, the R value for the moisture content was close to the concentration of $CaCl_2$, which were obviously greater than the ratio of $CaCl_2$ to urea. It indicated that the moisture content and the concentration of $CaCl_2$ showed similar effect significance on the UCS of PMMRS, while the concentration ratio of $CaCl_2$ to urea showed the lowest significance.

$$R=\max\{K_1, K_2, K_3, K_4, K_5\}-\min\{K_1, K_2, K_3, K_4, K_5\} \quad (7)$$

Based on the test results, variance analysis was also conducted to quantitatively investigate the effect significance of parameters of MICP process on the UCS of PMMRS, and the results are shown in Table 5. Since each parameter has five different levels, the degree of freedom was determined as four. Generally, the greater F-Value indicates that the parameter shows more significance for the evaluation index. The significance order of the parameters was the moisture content of the CLS (dry density), the concentration

of $CaCl_2$, and the concentration ratio of $CaCl_2$ to urea in cementation solution, respectively. The results demonstrated that moisture content and concentration of $CaCl_2$ showed a more significant effect on the UCS of PMMRS than the concentration ratio of $CaCl_2$ to urea, which was in accordance with the results in Table 4.

Table 5. The orthogonal experiment result analysis

Source of Variation	Sum of Squares of Separation	Degree of Freedom	Mean Square
Moisture content	76.48	4	19.12
Concentration of $CaCl_2$	68.98	4	17.25
Ratio of $CaCl_2$ to urea	10.14	4	2.54
Errors	29.99	12	2.50

In order to validate the effectiveness of orthogonal experiment, UCS test was performed on an additional groups of specimens, which were prepared according to the optimum parameters determined by the orthogonal experiment. The average UCS strength for the additional groups was 15.92 MPa,which was higher than all orthogonal experiment groups. It testified that the optimum parameters obtained by the orthogonal experiment can be used to prepare PMMRS with the greatest UCS strength.

3.2 Stress-Strain Characteristics of PMMRS in UCS Test

To study the mechanical characteristic of PMMRS, UCS test was performed on the PMMRS and simple mixing MICP reinforced soil (SMMRS) specimens. The PMMRS specimens were prepared according to the optimum parameters obtained by the orthogonal experiment. Additionally, the pure CLS, the bacteria solution, and the cementation solution were used to prepare the SMMRS specimen. Additionally, the SMMRS group's solutions have half the volume respectively and the same concentration as the solutions in the PMMRS group. In addition, pure CLS specimens with 9% moisture content were also prepared and tested as the control group. During the UCS test process, both the stress applied to the specimens and the corresponding strain was ~~recorded, and the results are shown in~~ Figure 4.

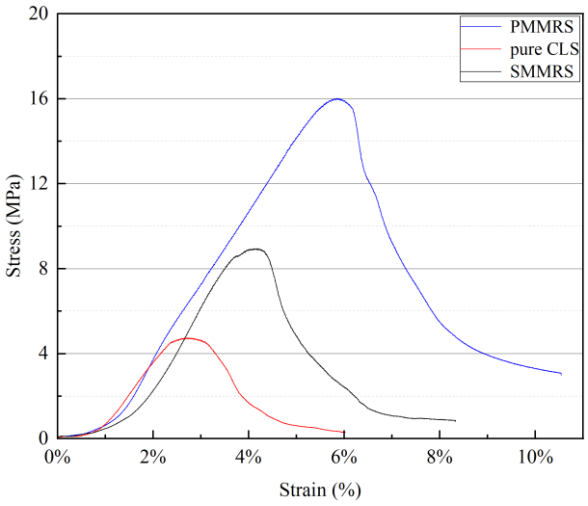


Figure 4. The strain-stress curve of PMMRS, SMMRS and pure CLS

As ~~shown in Figure 4, the~~ average UCS for the PMMRS group was the greatest, which was 15.92MPa, while the corresponding results for the SMMRS and pure CLS

specimens were 8.92MPa and 4.72MPa, respectively. The average UCS of the PMMRS group was almost 3 times than the pure CLS and increased by 78% than the SMMRS group. Moreover, the displacements under the peak stress for the PMMRS specimens were greater than the pure CLS and SMMRS. Results implieded that the pretreatment-mixing MICP method exhibit a higher improvement over the simple mixing MICP method.

3.3 UU Test

Figure 5 presents the shear response for the PMMRS, SMMRS and pure CLS specimens under a fixed stress of 100 kPa. For the UU test, the PMMRS specimens were prepared with the optimum parameters determined by the orthogonal experiment, and the pure CLS specimens were prepared with the same moisture content of 9%. As shown in Figure 5, the deviatoric stress for the MICP reinforced specimen was obviously greater than the pure CLS at the same axial strain, and the peak deviatoric stress increased with the increase in reinforcement effect. In addition, there were difference in the shear response among the PMMRS, SMMRS and pure CLS specimens. For the PMMRS specimen, the deviatoric stress initially increased with the axial strain and then tended to decrease after reaching the peak deviatoric stress. From this point of view, the strain-shear pressure response of PMMRS could be considered as the strain softening. Moreover, the corresponding response for the pure CLS was strain hardening. The deviatoric stress continually increased with the axial strain, and there was no peak stress appearing. For the SMMRS specimens, the strain-shear pressure response was between strain hardening and strain softening. The reason for this phenomenon might be the influence of MICP reinforcement effect. Montoya [30] found that the stress-strain response of specimens transitioned from strain hardening to strain softening with the MICP reinforcement effect. According to the results in section 3.2, the MICP reinforcement effect of PMMRS was superior to SMMRS. Therefore, the stress-strain response of PMMRS was strain hardening, and the response of SMMRS was between strain hardening and strain softening.

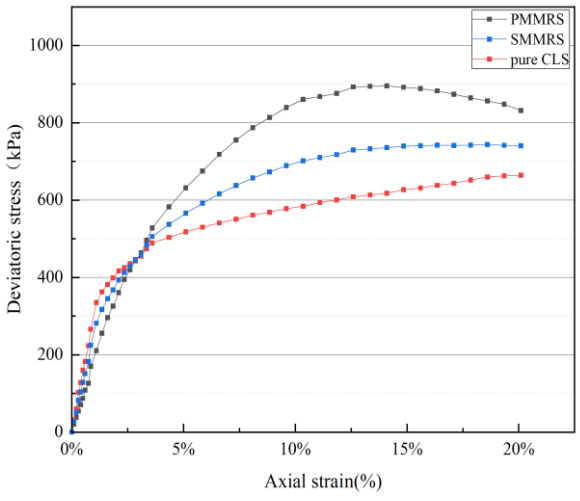
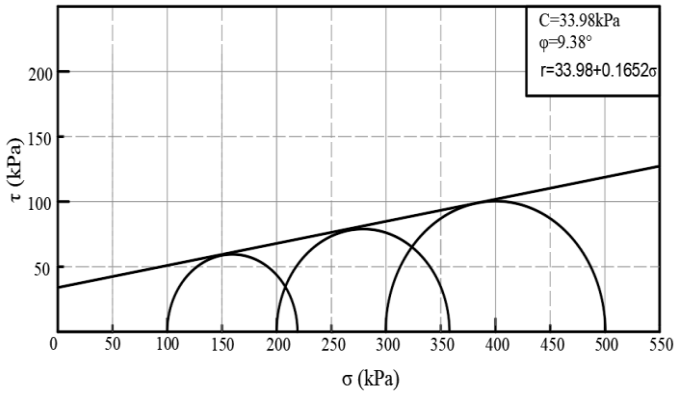


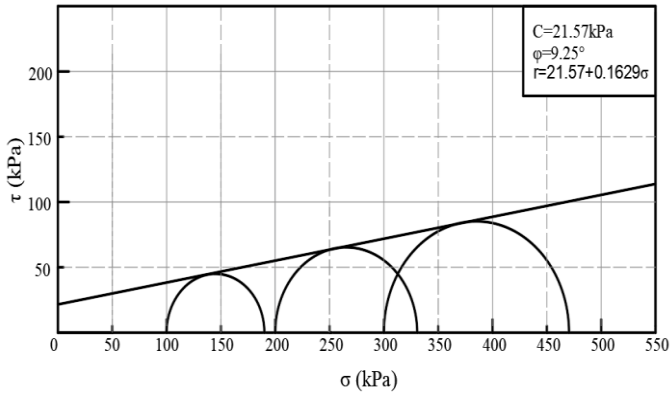
Figure 5. Shear response of specimens at confining pressure of 100 kPa

Moreover, Shear strength envelope for the PMMRS, SMMRS and pure CLS were obtained ~~and the results are shown in Figure 6.~~ The friction angle for the PMMRS, SMMRS and pure CLS specimens were 9.38°, 9.25° and 8.55°, while the cohesion values were 33.98 kPa, 21.57kPa and 14.54 kPa, respectively. As published by Mingjuan Cui [31] and Ivanov Volodymyr [32], the reinforcement mechanism of MICP on the soil can be summarized as two types of principles: bio-clogging and bio-cementation. On the one hand, the $CaCO_3$ crystals attach on the soil particles and improve the surface roughness,

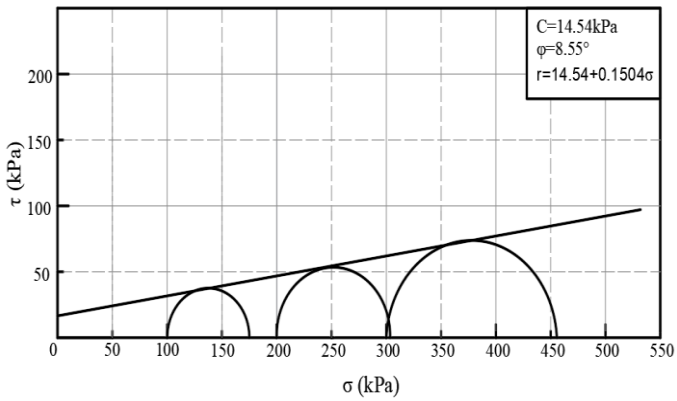
which increased the friction angle of the soil. On the other side, the $CaCO_3$ crystals could also bond soil particles together and hence improve the cohesion of the soil. Compare with the pure CLS, the cohesion of PMMRS and SMMRS showed a significant improvement while the friction angle increased by only 0.83° and 0.7°, respectively. It can be concluded that the bio-cementation principle mainly contributes to reinforcement effect for the mixing MICP method. Furthermore, both the friction angle and cohesion of PMMRS were greater than SMMRS, which also indicated that the pretreatment procedure could improve the reinforcement effect of the mixing MICP method.



(a)



(b)



(c)

Figure 6. Shear strength envelope of UU test. (a)PMMRS (b)SMMRS (c)pure CLS

3.4 $CaCO_3$ Distribution Characteristics

There is no doubt that the reinforcement effect of MICP on the soil is strongly dependent on the amount and distribution of $CaCO_3$ generated. In fact, it is really a great challenge that $CaCO_3$ is generated unevenly in the specimen, no matter the laboratory experiment or the field test [22]. Figure 7 presents the $CaCO_3$ content (CCC) test results of PMMRS and SMMRS in different sampling locations, which was detailed described in section 2.5.3. The CCC of PMMRS was greater than SMMPRS, while there was obvious difference in the CCC for different locations of both PMMRS and SMMRS specimens.

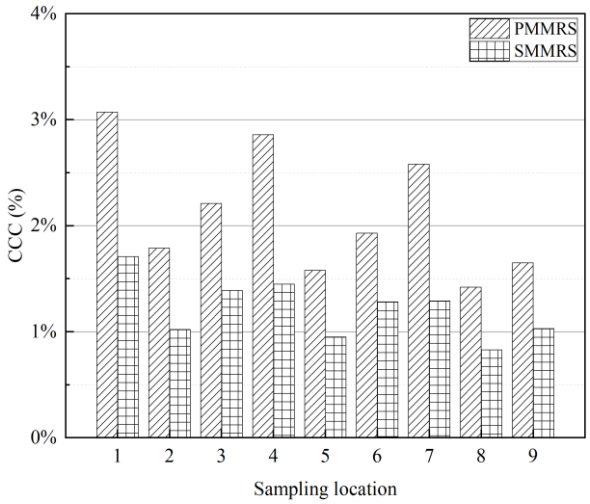


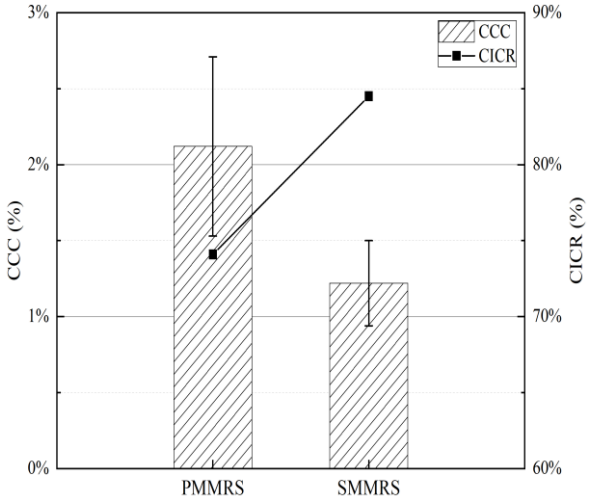
Figure 7. CCC test results of PMMRS and SMMRS in different sampling locations

Moreover, the average CCC for the specimen was used to study the relationship between the CCC in specimens and the $CaCl_2$ concentration in cementation solution. The calcium ion conversion rate was adopted to evaluate the efficiency of MICP process, which can be calculated by Eq. (8) and (9). The results of average CCC and calcium ion conversion rate (CICR) in different specimens are shown in Figure 8.

$$CCC_{max} = \frac{\mathrm{m}_a * \frac{9\%}{1000} * 3.0 * 100.09}{m_a} * 100\% \quad (8)$$

$$\mathrm{CICR} = \frac{CCC}{CCC_{max}} \quad (9)$$

where CCC_{max} is the theoretical maximum CCC in specimen.



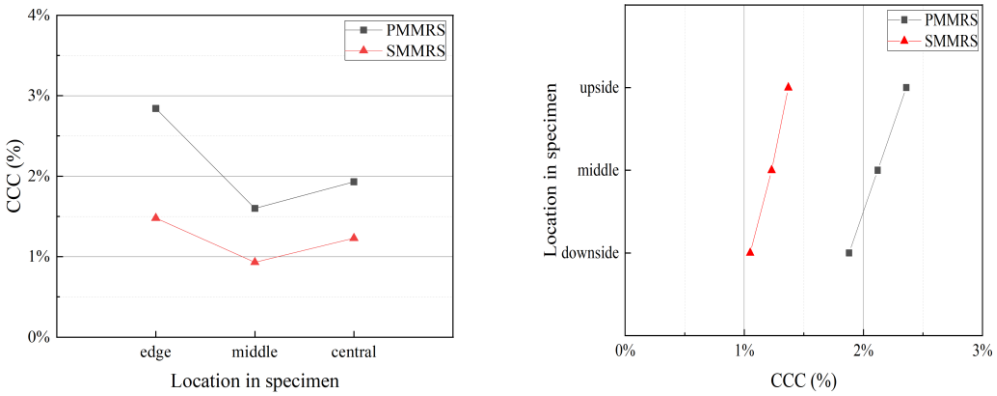
337 **Figure 8.** The average CCC and CICR of PMMRS and SMMRS

338 ~~Figure 8 illustrates that the~~ average CCC of PMMRS was increased by 74% than the
339 SMMRS while SMMRS had a higher CICR. Compared to the simple mixing MICP
340 method, pretreatment-mixing MICP method could provide two times of calcium ion for
341 mineralized bacteria to generate $CaCO_3$ theoretically. Therefore, PMMRS could have
342 higher CCC and better mechanical properties. However, excessive calcium ion could al-
343 so decrease the activity of urease in bacteria solution and attenuates the efficiency for
344 urea hydrolysis. Consequently, PMMRS would have lower CICR.
345 In this study, the distribution characteristics of $CaCO_3$ in both lateral and vertical
346 directions were studied as well. The CCC in different parts was calculated by averaging
347 the CCC of sampling locations as the corresponding column or line in Table 6. For ex-
348 ample, the CCC of the edge part was the average CCC of sampling locations 1, 4, and 7;
349 while the CCC of the downside part was the average CCC of sampling locations 7, 8,
350 and 9.

351 **Table 6.** The calculating strategy of $CaCO_3$ distribution characteristic

Direction		Lateral	
	Location	Edge	Middle
Vertical	Upside	1	2
	Middle	4	5
	Downside	7	8

352 The results of $CaCO_3$ distribution in the lateral and vertical directions are shown in
353 Figure 9. $CaCO_3$ distribution patterns for PMMRS and SMMRS were approximately sim-
354 ilar. In the lateral direction, the CCC of the edge part was the greatest, followed by the
355 central part and the middle parts. In the vertical direction, the CCC of the specimen
356 showed a decrease trend from the top to the bottom. The reason might be attributed to
357 the effect of oxygen on the mineralized bacteria. Sporosarcina pasteurii is a kind of mi-
358 croaerobic microorganism, which requires oxygen to survive and reproduce. The corre-
359 sponding mineralization reaction is considerably affected by the oxygen. Jain Surabhi
360 [33] reported that the urease activity and the amount of $CaCO_3$ formed by the Sporo-
361 sarcina pasteurii in the anaerobic condition is more negligible than the aerobic condition.
362 In addition, the dissolved oxygen in solution could influence the UCS and the $CaCO_3$
363 distribution in specimens [34]. For the Sporosarcina pasteurii, there are three ways to
364 obtain the oxygen in the PMMRS specimen, including the dissolved oxygen in solution,
365 oxygen existed in the pore, and the oxygen from outside environment. Generally, it is
366 hard for the bacteria inside the specimens to obtain the oxygen from the environment as
367 far away from the surface. Therefore, once the oxygen in solution and pore were con-
368 sumed completely, the mineralized bacteria could no longer survive, reproduce, and
369 generate $CaCO_3$. Consequently, CCC of edge part was the greatest in the lateral direction
370 while CCC decreased from the top to the bottom in the vertical direction.



(a) **(b)**

Figure 9. $CaCO_3$ distribution in PPMRS and SMMRS (a) lateral direction and (b) vertical direction

3.5 Curing time

In order to study the strength development of PMMRS, specimens were prepared and cured in a microbial incubator at 30°C for 1, 3, 5, 7, 14, 21, and 28 days, respectively. Then, the specimens were performed the UCS test after dried at 105°C for 24h. The UCS growth rate was defined and calculated by Eq. (10). The UCS and UCS growth rate for the PMMRS specimens within different curing periods are shown in Figure 10.

$$\text{UCS growth rate} = \frac{\text{UCS}_i}{\text{UCS}_{28d}} \times 100\% \quad (10)$$

Where UCS_i and UCS_{28d} are the average UCS of the PMMRS specimens cured for i days and 28 days, respectively, MPa.

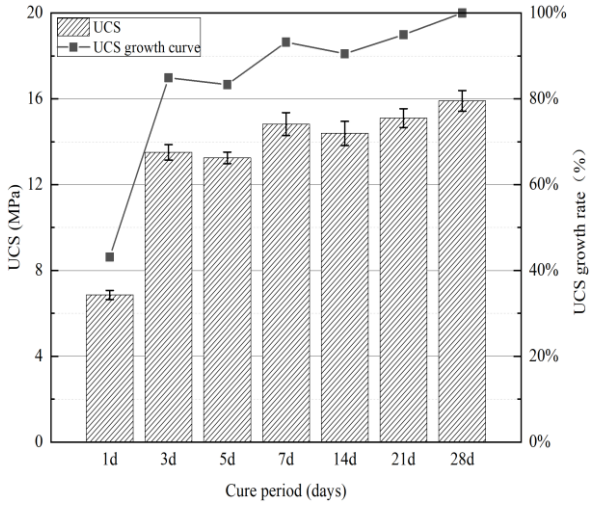


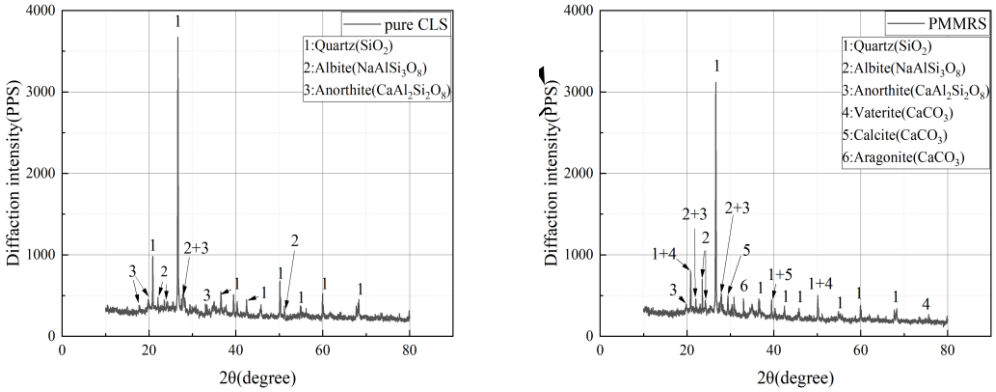
Figure 10. UCS development of PMMRS during the curing period

As shown in Figure 10, UCS of PMMRS increased within the whole curing period. It implied that the alive mineralized microorganisms continually consumed the cementation substances and nutrients, and produced the $CaCO_3$ to reinforce the CLS. Moreover, it was evident that the UCS development was strongly dependent on the curing period. After 1 day curing, the average UCS of PMMRS was 6.86MPa and the UCS growth rate was approximately 43% to the corresponding results of specimens cured for 28 days. For the specimens cured for 3 days, the average UCS was increased almost 2 times than the specimens cured for 1 day, and the corresponding UCS growth rate was 85%. In the

rest curing period, the UCS increased steadily, but the UCS improvement was relatively small. From this point of view, 3 days could be determined as the curing time for PMMRS specimen before test.

3.6 XRD Test

Figure 11 presents the X-ray diffraction test results for the pure CLS and PMMRS. There were three kinds of mineral components in the pure CLS sample, including the quartz, albite, and anorthite. Compare to the pure CLS sample, $CaCO_3$ was generated by the MICP process to reinforce the CLS. However, it was notable that there were three types of $CaCO_3$ in PMMRS sample, including vaterite, calcite, and aragonite. Due to the difference in crystal structures, these $CaCO_3$ products might show different reinforcement effect on the CLS. Therefore, further study is needed to determine the generation mechanisms and reinforcement effect of the $CaCO_3$ products in PMMRS.



(a) **(b)**

Figure 11. The XRD results of (a) pure CLS and (b) PMMRS

3.7 FESEM Test

Figure 12 and Figure 13 are the FESEM imagines for the pure CLS and the PMMRS specimens, respectively. For the pure CLS, small soil particles gathered and formed on the big particles in Figure 12 (a). As shown in Figure 12(b), $CaCO_3$ crystals were easily observed for the PMMRS specimen. Firstly, $CaCO_3$ crystals could bond the little soil particles together and thus increases the cohesion of the CLS. Moreover, some $CaCO_3$ crystals were attached to the surface of soil particles, which improves the internal friction between the soil particles. Therefore, the PMMRS specimens showed greater cohesion and friction angle than the pure CLS and hence contributes to greater strength, which was in accordance with the results of UCS and UU tests. Moreover, Figure 13 illustrates that three $CaCO_3$ crystals including calcite, aragonite and vaterite, were generated in PMMRS, which showed obvious differences in the morphology features. This was in accordance with the results in section 3.6. The rules for $CaCO_3$ generation and the effect mechanism on PMMRS are needed to be seriously clarified from the micro structural point of view in the future study.

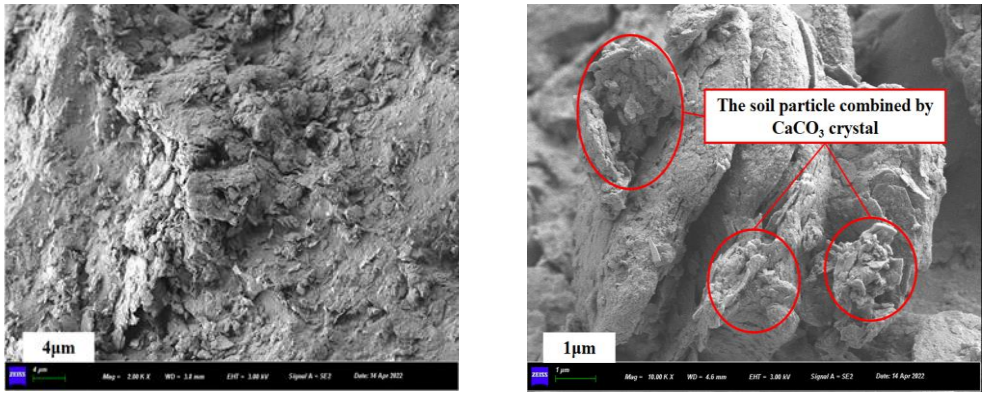


Figure 12. FESEM imagines of (a) pure CLS and (b) PMMRS

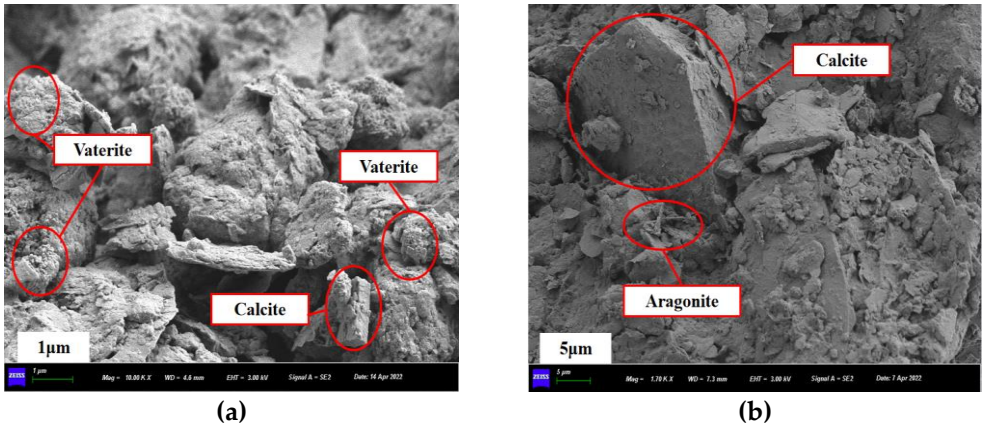


Figure 13. Different $CaCO_3$ crystal morphology of PMMRS

3.8 MIA Test

The MIA test results are shown in Figure 14 and Figure 15. As shown in Figure 14, for the small pore size, the pore volumes of the PMMRS and SMMRS were less than the pure CLS, while the results for the large pore size were the opposite. Figure 15 presents that PMMSR had the highest average pore diameter but lowest calculated porosity, while pure CLS did the opposite.

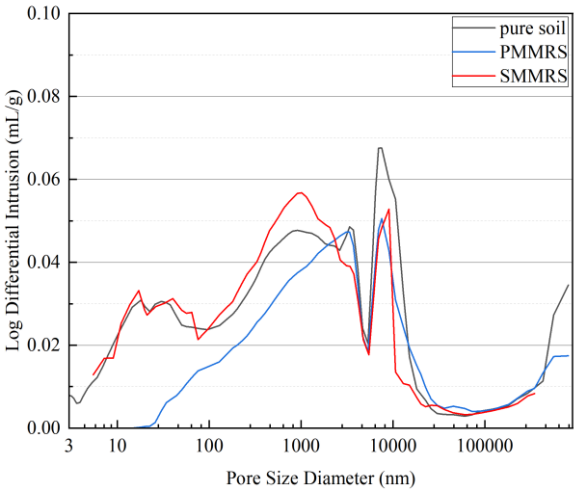


Figure 14. The pore distribution and volume of PMMRS, SMMRS and pure CLS

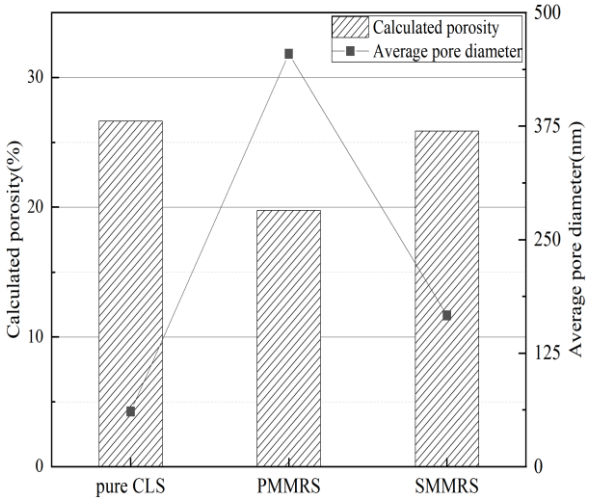


Figure 15. The calculated porosity and average pore diameter of PMMRS, SMMRS and pure CLS

The variations of cumulative intrusion and average pore diameter could be attributed to the $CaCO_3$ crystals generated in MICP reinforced soil. Due to the blocking effect of the $CaCO_3$ crystals, the proportions of pore with little size for all the MICP reinforced soil were smaller than the pure CLS. Since the small soil particles could be bonded together, the amount of little particle would be decreased and leading the pore filled with the little particles to be unblocked. Therefore, the average pore diameter in MICP reinforced soil would be increased. Referring to the UCS results of section 3.2, the UCS of specimens increased with the decrement of the calculated porosity as well as the increment of the average pore diameter. It can be concluded that the reinforcement effect of MICP reinforced soil was highly related to the pore structure of the soil.

4. Conclusions

The present work aimed to propose a strategy for mixing MICP method incorporated with the pretreatment procedure to stabilize the soil in road construction project. A series of laboratory tests were performed to investigate the preparation parameters, the engineering properties, the distribution characteristics of $CaCO_3$ as well as the mineralogy and micro structure of PMMRS. The key findings and recommendations drawn from the study are listed below:

(1) The orthogonal experiment results determined the optimum parameters for preparing PMMRS, i.e., moisture content of 9%, the concentration of $CaCl_2$ 3.0 mol/L, and the concentration ratio of $CaCl_2$ to urea 1:1. The moisture content and the concentration of $CaCl_2$ showed the significant effect on the UCS of PMMRS. In contrast, the effect of the concentration ratio of $CaCl_2$ to urea was relatively low.

(2) The pretreatment procedure could significantly improve the reinforcement effect of mixing MICP method on the CLS. Compared to the pure CLS and SMMRS specimen, the UCS of PMMRS specimen was increased by 198% and 78%, respectively. The reinforcement effect could be attributed to improvement of cohesion of the soil. Moreover, the mineralization reaction would affect the pore structure of the soil, which was highly related to the reinforcement effect of MICP reinforced soil

(3) For the pretreatment-mixing MICP method, mineralization reaction would last for a period, leading the UCS of PMMRS increased continually. After 3 days curing, the UCS growth rate of the specimens increased rapidly to 85% of the specimens cured for 28days. Therefore, 3 days was recommended as the curing time for PMMRS specimen before performing the test.

(4) The $CaCO_3$ distribution inside the specimen was not so evenly no matter the lateral or vertical direction. The CCC of edge part was the greatest in the lateral direction

while decreased from the top to the bottom in the vertical direction. The reason might be attributed to the effect of oxygen on the mineralized bacteria. However, the strength of PMMRS was not monotonously positively related to the CCC with the increment of the $CaCl_2$ concentration.

To facilitate the application of pretreatment-mixing MICP method, further research can be conducted on the generation mechanisms and reinforcement effect of different $CaCO_3$ products in PMMRS. Moreover, it is strongly recommended to investigate the methodology for making the $CaCO_3$ generated evenly in the PMMRS. Furthermore, long-term performance of PMMRS is also needed to be investigated in order to verify the indoor test results in further studies.

Author Contributions: Conceptualization, X.H.; methodology, X.H., X.F. and P.P.; investigation, X.F., L.L. and Y.S.; resources, X.H.; data curation, X.F. and L.L.; writing—original draft preparation, X.F.; writing—review and editing, P.P. and Y.S.; supervision, X.H. and P.P.; project administration, X.H.; funding acquisition, P.P. and Y.S. All authors have read and agreed to the published version of the manuscript.

Funding: This research was funded by Technology Project of Department of Transportation of Hubei Province (No. 2022-11-1-2), the Nature Science Foundation of Hubei Province (No. 2019CFB330), and the Zhejiang Provincial Natural Science Foundation (No. LGG21E080002).

Institutional Review Board Statement: Not applicable.

Informed Consent Statement: Not applicable.

Data Availability Statement: All the data in the tests of this study have been listed in the paper.

Acknowledgments: In this section, you can acknowledge any support given which is not covered by the author contribution or funding sections. This may include administrative and technical support, or donations in kind (e.g., materials used for experiments).

Conflicts of Interest: The authors declare no conflict of interest.

References

1. Zadehmohamad, M.; Luo, N.; Abu-Farsakh, M.; Voyiadjis, G. Evaluating long-term benefits of geosynthetics in flexible pavements built over weak subgrades by finite element and Mechanistic-Empirical analyses. Geotext. Geomembr. 2022, 50, 455-469, doi:10.1016/j.geotexmem.2022.01.004.
2. Abdizadeh, D.; Pakbaz, M.S.; Nadi, B. Numerical Modeling of Lateral Dynamic Compaction on the Slope in Dry Sand. KSCE Journal of Civil Engineering 2020, 25, 398-403, doi:10.1007/s12205-020-2344-8.
3. Saleh, S.; Yunus, N.Z.M.; Ahmad, K.; Ali, N. Improving the strength of weak soil using polyurethane grouts: A review. Construction and Building Materials 2019, 202, 738-752, doi:10.1016/j.conbuildmat.2019.01.048.
4. Yoon, K.B.; Ryu, H.M.; Lee, G.H.; Gopalan, A.I.; Sai-anand, G.; Lee, D.E. Enhanced compressive strength of rammed earth walls stabilized with eco-friendly multi-functional polymeric system. Renew. Sust. Energ. Rev. 2021, 152, 111681, doi:10.1016/j.rser.2021.111681.
5. Liu, L.; Deng, T.; Deng, Y.; Zhan, L.; Horpibulsuk, S.; Wang, Q. Stabilization nature and unified strength characterization for cement-based stabilized soils. Construction and Building Materials 2022, 336, 127544, doi:10.1016/j.conbuildmat.2022.127544.
6. Miraki, H.; Shariatmadari, N.; Ghadir, P.; Jahandari, S.; Tao, Z.; Siddique, R. Clayey soil stabilization using alkali-activated volcanic ash and slag. Journal of Rock Mechanics and Geotechnical Engineering 2022, 14, 576-591, doi:10.1016/j.jrmge.2021.08.012.
7. Benhelal, E.; Zahedi, G.; Shamsaei, E.; Bahadori, A. Global strategies and potentials to curb CO2 emissions in cement industry. Journal of cleaner production 2013, 51, 142-161, doi:10.1016/j.jclepro.2012.10.049.
8. Eliasson, B.; Riemer, P.; Wokaun, A. Greenhouse gas control technologies; Elsevier: 1999.
9. Konstantinou, C.; Wang, Y.; Biscontin, G.; Soga, K. The role of bacterial urease activity on the uniformity of carbonate precipitation profiles of bio-treated coarse sand specimens. Scientific reports 2021, 11, 6161, doi:10.1038/s41598-021-85712-6.

10. Peng, S.; Zhang, K.; Fan, L.; Kang, J.; Peng, K.; Wang, F. Permeability reduction and electrochemical impedance of fractured rock grouted by microbial-induced calcite precipitation. Geofluids 2020, 2020, 8876400, doi:10.1155/2020/8876400.
11. Liu, K.-W.; Jiang, N.-J.; Qin, J.-D.; Wang, Y.-J.; Tang, C.-S.; Han, X.-L. An experimental study of mitigating coastal sand dune erosion by microbial-and enzymatic-induced carbonate precipitation. Acta Geotechnica 2021, 16, 467-480, doi:10.1007/s11440-020-01046-z.
12. Liu, S.; Du, K.; Huang, W.; Wen, K.; Amini, F.; Li, L. Enhanced erosion resistance of cement-treated bricks using multiple biological surface treatments. Advances in Cement Research 2021, 33, 540-549, doi:10.1680/jadcr.20.00024.
13. Liu, J.; Li, G.; Li, X.a. Geotechnical engineering properties of soils solidified by microbially induced CaCO3 precipitation (MICP). Advances in Civil Engineering 2021, 2021, 6683930, doi:10.1155/2021/6683930.
14. Chen, P.; Zheng, H.; Xu, H.; Gao, Y.-x.; Ding, X.-q.; Ma, M.-l. Microbial induced solidification and stabilization of municipal solid waste incineration fly ash with high alkalinity and heavy metal toxicity. PloS One 2019, 14, e0223900, doi:10.1371/journal.pone.0223900.
15. Van Paassen, L.A.; Daza, C.M.; Staal, M.; Sorokin, D.Y.; van der Zon, W.; van Loosdrecht, M.C. Potential soil reinforcement by biological denitrification. Ecological Engineering 2010, 36, 168-175, doi:10.1016/j.ecoleng.2009.03.026.
16. Wang, H.; Miao, L.; Sun, X.; Wu, L.; Fan, G. Experimental Study of Enzyme-Induced Carbonate Precipitation for High Temperature Applications by Controlling Enzyme Activity. Geomicrobiology Journal 2022, 10.1080/01490451.2022.2045649, 1-13, doi:10.1080/01490451.2022.2045649.
17. Song, M.; Ju, T.; Meng, Y.; Han, S.; Lin, L.; Jiang, J. A review on the applications of microbially induced calcium carbonate precipitation in solid waste treatment and soil remediation. Chemosphere 2022, 290, 133229, doi:10.1016/j.chemosphere.2021.133229.
18. Tiwari, N.; Satyam, N.; Sharma, M. Micro-mechanical performance evaluation of expansive soil biotreated with indigenous bacteria using MICP method. Scientific Reports 2021, 11, 1-12, doi:10.1038/s41598-021-89687-2.
19. Wang, L.; Wang, X.; Li, F.; Cui, M.; Yang, X.; Yang, M.; Yan, Y. Advances of enzymes related to microbial cement. Chinese Journal of Biotechnology 2022, 38, 506-517, doi:10.13345/j.cjb.210127.
20. DeJong, J.T.; Fritzges, M.B.; Nüsslein, K. Microbially induced cementation to control sand response to undrained shear. Journal of geotechnical and geoenvironmental engineering 2006, 132, 1381-1392, doi:10.1061/ASCE1090-0241(2006)132:11(1381).
21. Kannan, K.; Bindu, J.; Vinod, P. Engineering behaviour of MICP treated marine clays. Marine Georesources & Geotechnology 2020, 38, 761-769, doi:10.1080/1064119X.2020.1728791.
22. Xiao, Y.; Xiao, W.; Ma, G.; He, X.; Wu, H.; Shi, J. Mechanical Performance of Biotreated Sandy Road Bases. Journal of Performance of Constructed Facilities 2022, 36, 04021111, doi:10.1061/(ASCE)CF.1943-5509.0001671.
23. Liu, S.; Wen, K.; Armwood, C.; Bu, C.; Li, C.; Amini, F.; Li, L. Enhancement of MICP-treated sandy soils against environmental deterioration. J Mater Civil Eng 2019, 31, 04019294, doi:10.1061/(ASCE)MT.1943-5533.0002959.
24. Porter, H.; Dhami, N.K.; Mukherjee, A. Sustainable road bases with microbial precipitation. Proceedings of the Institution of Civil Engineers-Construction Materials 2018, 171, 95-108, doi:10.1680/jcoma.16.00075.
25. Xiao, J.; Wei, Y.; Cai, H.; Wang, Z.; Yang, T.; Wang, Q.; Wu, S. Microbial-induced carbonate precipitation for strengthening soft clay. Advances in Materials Science and Engineering 2020, 2020, 8140724, doi:10.1155/2020/8140724.
26. Lu, T.; Wei, Z.; Wang, W.; Yang, Y.; Cao, G.; Wang, Y.; Liao, H. Experimental Investigation of sample preparation and grouting technology on microbially reinforced tailings. Construction and Building Materials 2021, 312, 125458, doi:10.1016/j.conbuildmat.2021.125458.
27. Zamani, A.; Montoya, B. Undrained monotonic shear response of MICP-treated silty sands. Journal of Geotechnical and Geoenvironmental Engineering 2018, 144, 04018029, doi:10.1061/(ASCE)GT.1943-5606.0001861.
28. Rebata-Landa, V. Microbial activity in sediments: effects on soil behavior. Georgia Institute of Technology, 2007.
29. Choi, S.-G.; Park, S.-S.; Wu, S.; Chu, J. Methods for calcium carbonate content measurement of biocemented soils. J. Mater. Civ. Eng 2017, 29, 06017015, doi:10.1061/(ASCE)MT.1943-5533.0002064.
30. Montoya BM, DeJong JT (2015) Stress–strain behavior of sands cemented by microbially induced calcite precipitation. J Geotech Geoenviron Eng 141(6):04015019, doi: 10.1061/(ASCE)GT.1943-5606.0001302.
31. Cui, M.-J.; Zheng, J.-J.; Zhang, R.-J.; Lai, H.-J.; Zhang, J. Influence of cementation level on the strength behaviour of bio-cemented sand. Acta Geotechnica 2017, 12, 971-986, doi:10.1007/s11440-017-0574-9.

566 32. Ivanov, V.; Chu, J. Applications of microorganisms to geotechnical engineering for bioclogging and biocementa-
567 tion of soil in situ. Reviews in Environmental Science and Bio/Technology 2008, 7, 139-153,
568 doi:10.1007/s11157-007-9126-3.
569 33. Jain, S.; Arnepalli, D. Biochemically induced carbonate precipitation in aerobic and anaerobic environments by
570 Sporosarcina pasteurii. Geomicrobiology Journal 2019, 36, 443-451, doi:10.1080/01490451.2019.1569180.
571 34. Li, M.; Wen, K.; Li, Y.; Zhu, L. Impact of oxygen availability on microbially induced calcite precipitation (MICP)
572 treatment. Geomicrobiology Journal 2018, 35, 15-22, doi:10.1080/01490451.2017.1303553.

573